Abstract for the 10th International Workshop on Water Waves and Floating Bodies, Oxford, U.K., April 2–5, 1995.

UNSTEADY WAVES NEAR A VERTICAL CIRCULAR CYLINDER IN A VISCOUS FLUID

Ronald W. Yeung and Xing Yu
Department of Naval Architecture and Offshore Engineering
University of California at Berkeley, Berkeley, CA 94720-1780, USA.

Background. The hydrodynamic interaction of surface waves with marine structures has always been of much interest to marine industry. In many applications, potential flow model can be an adequate predictive tool. Even so, there are many cases of practical interest when fluid viscosity is important. A traditional but empirical means of accounting for viscous effects is to use formulas such as Morison's equation [1] with pre-determined coefficients. The validity of such a procedure cannot be fully established even for the case of an infinite fluid. Aside from an interest derived from engineering applications, there exists also the basic need of understanding how viscosity may alter the behavior of the flow near a free surface, particularly in the neighborhood of a body boundary. In our ongoing effort to study such viscous flows near a free surface, we presented in the last Workshop [2], as a first step, a highly accurate spectral formulation for modeling inviscid wave-cylinder interaction. The potential of this method has now been further tapped and informative results for the case of a viscous fluid are now emerging. It is worthy to mention that there have been considerable recent advances in the inclusion of viscous effects in free-surface flows with a body (see e.g. [3], [4] and [5], [6] etc). Most of the above advances are restricted to two-dimensional problems. Because of the enormous computational demand on three-dimensional flows, a highly efficient method needs to be developed. Efficiency aside, it should also resolve the intricate flow details often associated with flow separation. The treatment we describe below has led to a fruitful direction of investigation.

Spectral methods have been frequently studied and applied to obtain solutions of many fluid dynamics problems (e.g. [7] and [8]). They are well known for efficiency and accuracy. Cylindrical geometry may be considered as one of the simpler shapes, and is therefore particularly appropriate for this type of solution method.

Problem Formulation and Numerical Procedure. As in [2], the fluid domain is taken to be a region between two vertical, concentric cylindrical surfaces, with the inner cylinder being considered as the body and the outer cylinder a closure boundary which can be taken at a large distance away from the inner one. Our formulation of the free-surface flow problem for a viscous fluid is based on primitive variables, and is similar to that given in [5]. The Navier-Stokes equations are complemented by one kinematic and three dynamic boundary conditions on the free surface, the latter representing the stress continuity relations. These boundary conditions are linearized for the present study.

The Navier-Stokes equations are solved using a fractional-step method. This is implemented in the spirit of a "projection method" [9] which involves, in the first half-step, solving for an intermediate auxiliary velocity field from the momentum equations without the pressure gradient term. Then in the second half-step, a Poisson equation for the pressure field is solved, utilizing the auxiliary velocity solved previously. The projection decomposition then leads to a correction of the auxiliary velocity to yield the true velocity field satisfying the field equations and boundary conditions.

The above numerical procedure is implemented in cylindrical coordinates using a pseudo-spectral method. Space limitation allows only a brief description here [10]. An ADI scheme [11] is first used to solve the momentum equations. With this scheme and the introduction of two additional intermediate auxiliary velocities, the three scalar momentum equations (three-dimensional partial differential equations) become nine ordinary differential equations (ODEs.) These resulting ODEs are next solved by using spectral collocation methods [7]. The pressure Poisson equation is then solved efficiently and accurately by the pseudo-spectral formulation presented in the last Workshop [2].

Analytical Validations. To validate our solution method, we apply two tests for which analytical solutions can be obtained. First, to show this method's ability to handle large-time simulations, we solve a cylindrical version of Stokes's second problem, corresponding to a cylinder rotating time-harmonically in a viscous fluid. Analytically, this turns out to be a one-dimensional problem, with the spatial factor of the circumferential velocity field expressible as a single function $f(r)$ of a "Reynolds-number modified" radial

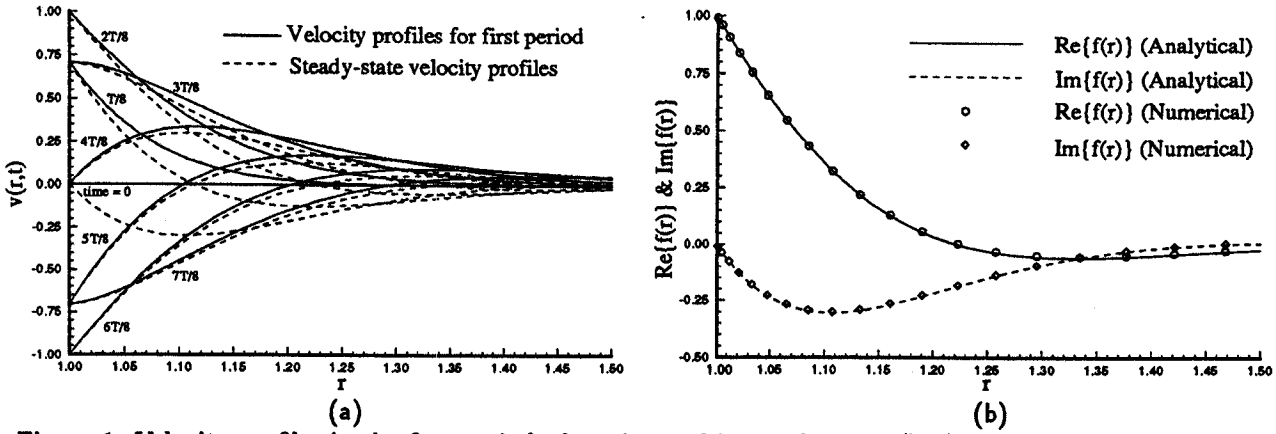

Figure 1: Velocity profiles in the first period of motion and in steady-state (left). Real and imaginary parts of function $f(r)$ (right).

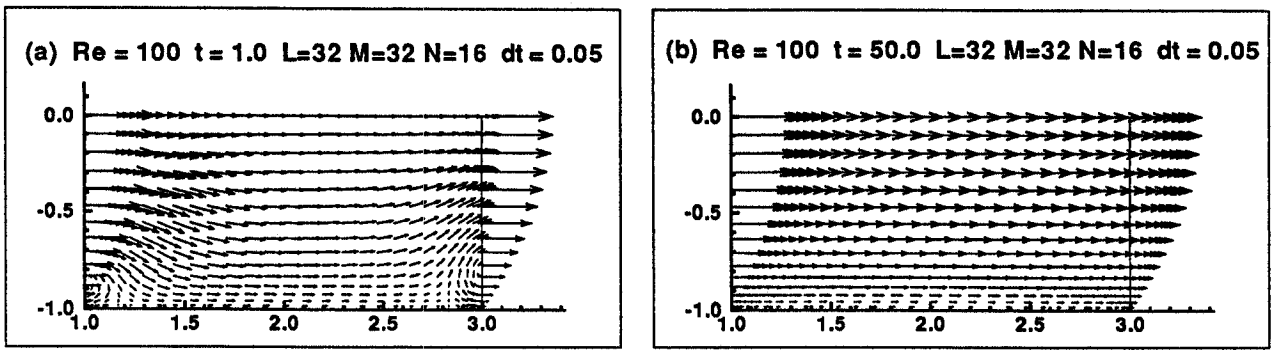

Figure 2: Velocity vectors in the plane $\theta = 0$ at $t = 1.0$ (a) and $t = 50.0$ (b).

coordinate r. As a stringent test, we solve numerically this problem as a fully three-dimensional *transient* problem. To simulate the desired physical conditions, free-slip boundary conditions are used on the top and bottom (horizontal) boundaries, as well as the (far-field) outer cylinder.

Fig. 1a shows a sample of the circumferential velocity profiles $v(r,t)$ at eight instants of time during the first period of oscillation and the corresponding limiting "steady-state" profile at the $7th$ cycle. Numerical results show that the transients are only significant during the first couple of cycles of oscillation. To show the accuracy of our numerical solution, we further plot in Fig. 1b a comparison of the real and imaginary parts of the analytical complex steady-state velocity function $f(r)$ with the numerical values. Excellent agreement is observed.

As a second test problem, we utilize the solution of a Poiseuille flow between two parallel surfaces, with the bottom surface being a no-slip and the top a free-slip boundary. Again, this is treated as a three-dimensional transient problem by the solution method discussed in the last section. This is accomplished by imposing quadratic Poiseuille velocity profiles onto *both* inner and outer cylinders as Dirichlet conditions for the velocity at time $t = 0$, and held constant thereafter. Further, a pressure field of constant gradient in the flow direction is applied on these cylindrical surface as a Dirichlet condition for pressure.

The numerical results for such a test are presented in Fig. 2, with the radius of the outer cylinder being three times the radius of the inner one. Velocity profiles are shown in the vertical plane of symmetry behind the inner cylinder, one (a) for an early time instant and the other (b) one for a large time. In Fig. 2a, the flow is rather transient, and two vortical structures are observed at two lower corners. Fig. 2b shows an almost steady flow, in which the velocity vectors everywhere in this plane are observed to have approached the Poiseuille velocity profile prescribed on the two cylindrical boundaries. A close examination of the numerical results reveals that a maximum difference between the value of velocity at any point in the domain and its expected steady-state value is less than 1% at time $t = 50.0$.

Viscous Free-Surface Flows: Results and Discussion. Having established our numerical method to be reliable and accurate, we proceed to include the genuine free-surface conditions on the top surface of the fluid. The Cauchy-Poisson wave problem as solved in [2] is now re-solved for the case of a *viscous* fluid. In such a problem, an initially still fluid is set to motion by releasing a prescribed free-surface hump at time $t = 0$. In order to understand the influence of viscosity, results for viscous flow are compared with their inviscid counterparts, where appropriate.

Numerical results, for both viscous and inviscid flows, are obtained by a mesh size of $L \times M \times N = 64 \times 64 \times 32$ (L, M and N denote the numbers of grids in radial, circumferential and vertical directions respectively for our spectral formulation). The Reynolds number Re, defined by cylinder radius a, gravitational acceleration g and viscosity ν as $\sqrt{ag}a/\nu$, is set as 10,000. The time step Δt, non-dimensionalized by $\sqrt{a/g}$, is chosen to be 0.05. The amplitude of the initial free-surface hump A, non-dimensionalized by a, is taken to be 0.1, and the center of the hump is placed at $r = 2.318$. The three-dimensional code was run for as long as 300 time steps. It was observed to be sufficiently long to allow the "main wave" to diffract around the cylinder.

There is an enormous wealth of information coming out of the solution of this type of problem. Some preliminary observations are discussed here. During the early stage of the simulation, viscosity is expected to play only a minor role; the early-time flow features of viscous and inviscid flows are therefore expected to be similar. This is evident from Fig. 3a, in which the free-surface elevations at $r = 1$ (body-free-surface intersection) and $r = 2.318$ (center of initial hump) are plotted as functions of time. Further, Fig. 3a shows that the waves damp out much sooner in a viscous fluid than in an inviscid fluid. This behavior can also be observed from the perspective views of the overall free surface pattern displayed in Fig. 4.

In Fig. 3b, we show the hydrodynamic forces acting on the circular cylinder for the cases of inviscid and viscous flows. It is apparent that, in the case of viscous flow, the only significant component is the horizontal force due to pressure, which varies with time in a similar fashion to its inviscid counterpart, except for a phase shift.

For a closer look at the viscous-flow patterns, we include a vorticity plot and a surface-contour plot as Figs. 5a–b. In Fig. 5a, the velocity vectors are overlaid onto a vorticity contour plot in the vertical plane of symmetry containing the initial wave peak. This figure corresponds to $t = 12.00$. Two vortices of opposite signs can be clearly seen near the intersection of the body and the free surface. A boundary layer immediately above the bottom is also observed. Fig. 5b shows the corresponding free-surface elevation contours. Also plotted are the velocity vectors on the free surface. It is of interest to note that the vorticity component *normal* to the free surface is vanishingly small (not shown) except near the body. This suggests that vortex structures generated by the surface motion are primarily parallel to the water surface. These and other data of an extensive nature will offer valuable insights for understanding vortical free-surface flows near a body. In the Workshop, these results will be discussed in depth, as well as the exciting potential of the present method for treating a host of other problems of practical interest.

References

1. Morison, J. R., O'Brein, M. P., Johnson, J. W. and Schaaf, S. A., *Petroleum Transaction*, Vol. 189, pp. 149-154.
2. Yeung, R. W. and Yu, X., *Proceedings of 9th Workshop on Water Waves and Floating Bodies*, Kuju, Oita, Japan, 1994, pp. 235-239.
3. Miyata, H., Toru, S. and Baba, N., *Journal of Computational Physics*, Vol. 72, 1987, pp. 393-421.
4. Yeung, R. W. and Wu, C. F., *Journal of Offshore Mechanics and Arctic Engineering*, Vol. 113, 1991, pp. 334-343.
5. Yeung, R. W. and Ananthakrishnan, P., *Proceedings of the 19th Symposium on Naval Hydrodynamics*, Seoul, South Korea, 1992.
6. Yeung, R. W. and Vaidhyanathan, M., *Proceedings of the International Conference on Hydrodynamics*, Wuxi, China, October 1994, pp. 118-128.
7. Gottlieb, D. and Orszag, S. A., *SIAM*, Philadelphia, PA., 1977.
8. Hussaini, M. and Zang, T., *Annual Review of Fluid Mechanics*, Vol. 19, 1987, pp. 339-367.
9. Chorin, A. J., *Studies on Numerical Analysis*, Vol. 2, 1968, pp. 64-71.
10. Yeung, R. W. and Yu, X., *Proceedings of 20th Symposium on Naval Hydrodynamics*, Santa Barbara, CA, 1994.
11. Goda, K., *Journal of Computational Physics*, Vol. 30, 1979, pp. 76-95.

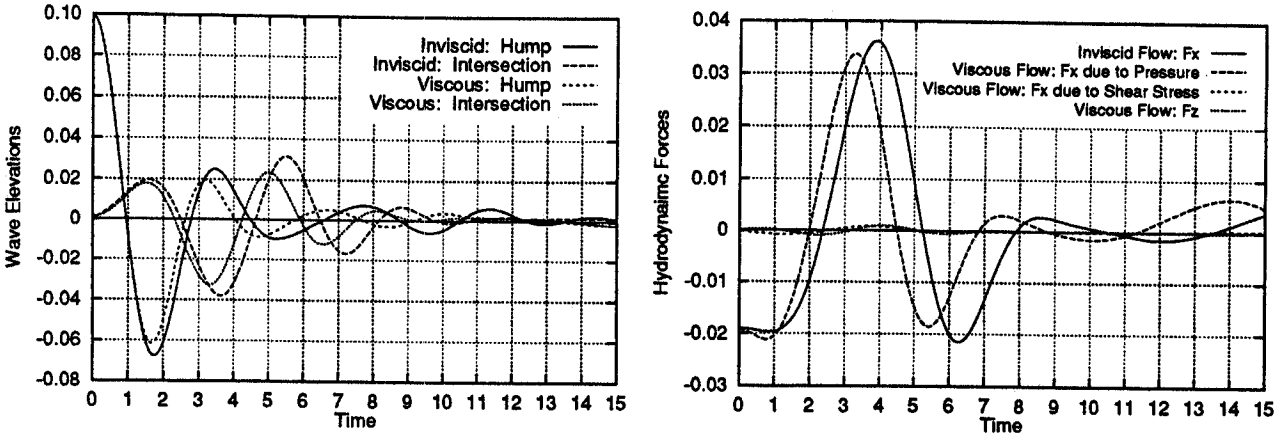

(a) (b)

Figure 3: Time histroy of wave elevation at $r = 1$ (body-free-surface intersection) and $r = 2.318$ (center of initial hump) in the vertical plane of symmetry behind the inner cylinder (left) and time history of hydrodynamic forces on cylinder (right).

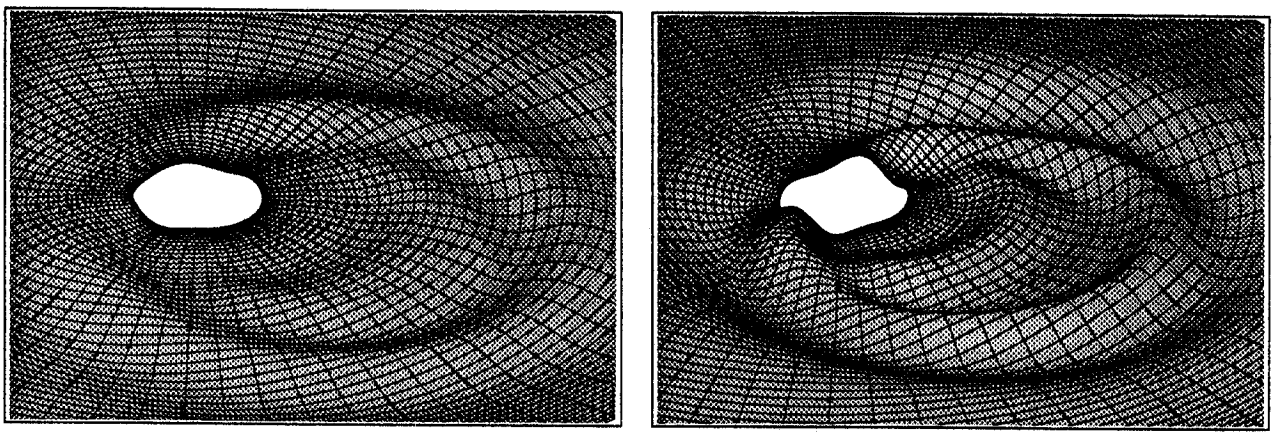

(a) (b)

Figure 4: Free-surface elevations for the cases of viscous flow (left) and inviscid flow (right) at $t = 12.00$.

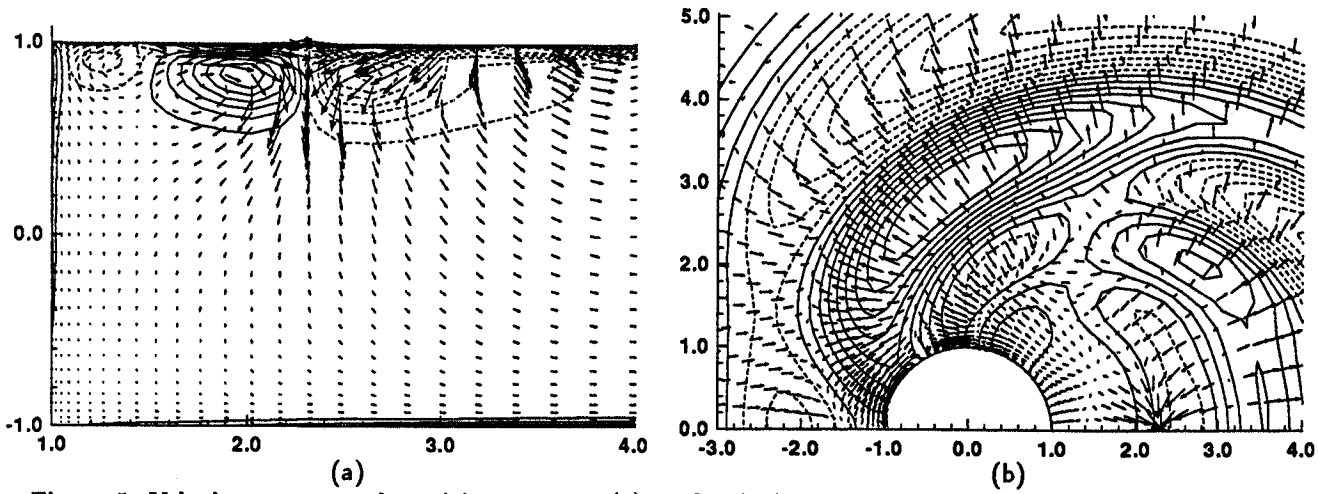

(a) (b)

Figure 5: Velocity vectors and vorticity contours (a), and Velocity vectors and vorticity contours (b) in the vertical plane of symmetry behind the inner cylinder at $t = 12.00$ (Dash-line represents counter-clockwise vorticity in (a) and negative elevation in (b)).